Advances in Biology & Earth Sciences
Vol.4, No.3, 2019, pp.150-175

IMPLICATIONS OF THE MODIFIABLE AREAL UNIT PROBLEM FOR WILDFIRE ANALYSES

Timothy Nagle-McNaughton[1*], Xi Gong[2], José A. Constantine[3]

[1]Department of Earth & Planetary Sciences, University of New Mexico, Albuquerque, NM 87131, USA
[2]Department of Geography & Environmental Studies, University of New Mexico, Albuquerque, NM 87131, USA
[3]Department of Geosciences, Williams College, Williamstown MA 01267, USA

Abstract. Wildfires pose a danger to both ecologies and communities. To this end, many large-scale analyses of wildfire patterns and behavior rely on the aggregation of point data to polygons, typically those based on distinct disparate ecological areas. However, the sizes, shapes, and orientations of the polygons to which data are aggregated are not neutral factors in the resulting analysis. The influence of the aggregation polygons on calculated results is known as the modifiable areal unit problem (MAUP), which is well-documented in the spatial statistics literature. Despite the documentation of the MAUP, relatively few wildfire studies consider the effects of the MAUP on their results. Here, wildfire data from the Western United States are aggregated to twenty-five different sets of polygons. Variation by fishnet polygon area and shape are measured via summary statistics and a spatio-temporal trend analysis. Variation is also quantified between well-established hierarchical nested ecoregion polygons via summary statistics. Lastly, best practices for mitigating the effects of the MAUP on future wildfire studies are recommended.

Keywords: *wildfires, spatial statistics, modifiable areal unit problem.*

Corresponding Author: *Timothy, Nagle-McNaughton, The University of New Mexico Earth and Planetary Sciences, MSCO3-2040, 1, University of New Mexico, Albuquerque, USA*
e-mail: timnaglemcnaughton@unm.edu

Received: *23 September 2019;* ***Accepted:*** *26 October 2019;* ***Published:*** *12 December 2019.*

1. Introduction

Human mismanagement of forests and alterations to the climate have caused wildfires to burn increasingly large areas across the US in the past three decades (Krawchuk *et al.*, 2009; Litschert *et al.*, 2012; Abatzoglou & Williams, 2016; Schoennagel *et al.*, 2017; Joseph *et al.*, 2018). The increase in wildfires has been met with greater efforts to control them. For example, between 1985 and 2017, total fire suppression costs increased from ~$200 million (2019 USD) to ~$3 billion (2019 USD), which exceeded the congressionally allocated funding in most recent years *(Calkin et al.*, 2005; Prestemon *et al.*, 2008; Abt *et al.*, 2009). To mitigate future damage, it is vital to understand the magnitude and rate of change in wildfire distribution spatially and temporally.

Many large-scale wildfire studies aggregate wildfire point data to polygons to enable broader correlations, predictions, and forecasts. These studies are based on large public databases of wildfire data such as the United States Forest Service Fire Program

Analysis Fire Occurrence Database (Short, 2017) and others[1]. Automated systems for detecting wildfires and updating databases have helped keep these datasets up-to-date and complete (Harris, 1996; Ambrosia *et al*., 1998; Feltz et al., 2003; Prins *et al*., 2003; Koltunov *et al.*, 2013).These databases generally contain point data representing each wildfire's ignition location, along with other fire attributes such as the total area burned, fire cause, date the fire was ignited, date the fire was contained, date the fire was extinguished, coordinates of the ignition location, and jurisdictional information. Data can then be aggregated to polygons and combined with other data relevant to the specific study, such as weather and climate data (Collins *et al.*, 2006; Westerling *et al*., 2006; Dennison *et al.*, 2014).

To generalize point-based analyses to areal conclusions, some form of aggregation to polygons is required. Ecoregions (or ecozones) are commonly used for this purpose in wildfire in studies in North America and Europe where such frameworks have been developed (Malamud *et al*., 2005; Jiang *et al.*, 2009; Jiang & Zhuang, 2011; Moreno *et al.*, 2011; Gralewicz *et al*., 2012; Litschert *et al*., 2012; Dennison *et al*., 2014; Fusco *et al.*, 2017; Fusco *et al*., 2018; Joseph *et al.*, 2018). In North America, these regions were first described in 1987 and were intended to delineate areas with disparate abiotic, biotic, and aquatic ecosystems by maximizing intra-zonal variation and minimize internal variation (Omernik, 1987). Since wildfires are strongly affected by the ecosystems in which they occurit is logical to use ecoregions as a categorical framework to analyzethe patterns of wildfire occurrence.

A larger hierarchical framework of nested ecoregions has been developed for North America since the original map was produced in 1987 by a collaboration of state and federal agencies and other partners to serve as a spatial framework for the research, assessment, management, and monitoring of ecosystems (McMahon *et al*., 2001; Omernik & Griffith, 2014). For example, the largest ecoregions are defined as Level I ecoregions, with smaller ecoregions defined as Level II. The original 1987 map was adapted into what are now the Level III ecoregions, and smaller sub-regions of the contiguous United States defined as Level IV ecoregions (McMahon *et al*., 2001; Omernik & Griffith, 2014). Although the framework of these regions is hierarchical, the ecoregions do not always nest perfectly, but are forced to nest for cartographic and database purposes (McMahon *et al*., 2001; Omernik, 2004; Omernik & Griffith, 2014).

Different ecoregion levels (and thus different polygon shapes and sizes) have been used for a variety of research purposes. However, the defined areas to which data are collected can have an effect on the resulting analysis. This connection has become known as the Modifiable Areal Unit Problem (MAUP) (Openshaw & Taylor, 1981; Openshaw, 1984; Fotheringham & Wong, 1991; Jelinski & Wu, 1996). The MAUP itself consists of two distinct but related problems: 1) the scale problem, and 2) the zoning problem. The scale problem results from the fact that relationships existing at onelevel of spatial analysis will not necessarily be the same strength at another level (Clark & Avery, 1976). Thus, if the same point/areal data were aggregated to different sizes of polygons, the resulting summary values could be different. In the zoning problem, resulting summary values could be different if the same point/areal data were aggregated to polygons of the same number but in different locations, orientations, or shapes.

[1] For example: the United States Federal Wildland Fire Occurrence Database (United States Department of Interior, 2018), the United States Monitoring Trends in Burn Severity Project (Finco *et al*., 2012), the Canadian National Fire Database (Canadian Forest Service, 2018).

The geographical and statistical literature has documented the effects of aggregating the same points to different polygons for more than 30 years (Clark & Avery, 1976; Perle, 1977; Openshaw & Taylor, 1981; Openshaw, 1984; Fotheringham, 1989; Fotheringham & Wong, 1991; Jelinski & Wu, 1996), but there was no consensus in the wildfire literature on which aggregation level to use. Malamud et al. (2005) used a three-level hierarchy developed by Bailey (1995) in which there are domains (based primarily on climate), divisions (climate, vegetation, and soils), and provinces (climate, vegetation, soils, land-surface form, and fauna) (Bailey, 1983, 1995). The Bailey divisions are most similar to the Level I or II Omernik ecoregions. Dennison et al. (2014) used the Omernik Level III ecoregions to study trends in large wildfires in the American West. Fusco et al. (2017) used the Omernik Level I ecoregions to study patterns of anthropogenic wildfires in the United States. Fusco et al. (2018) used the Omernik Level III ecoregions in a similar study of large anthropogenic wildfires in the United States. Joseph et al. (2018) used the Omernik Level III ecoregions in predicting extreme wildfires in the United States. Gralewicz et al. (2012) used the equivalent of Omernik Level II ecoregions to characterize the spatial and temporal patterns of wildfire ignitions in Canada (Ecological Stratification Working Group, 1995). Jiang et al. (2009) and Jiang and Zhuang (2011) used the same ecoregions as Gralewicz et al. to study wildfires in boreal forests in Canada.

Despite the near-universal acknowledgement of the MAUP in geospatial statistics and the development of best-practices for dealing with the MAUP, relatively few studies have considered the effects of the MAUP on wildfire data. However, the work of Fiorucci et al. (2008) demonstrated the MAUP affects the results of a popular technique for wildfire analysis, and that the MAUP should be further studied and considered. Fiorucci et al. characterized wildfire regimes under different areal partitioning schemes and found that the MAUP resulted in significantly different results for the power law parameters that characterize wildfire regime of a given area based on the work of Malamud et al. (2005). This study assesses the influence of the MAUP on the statistical analyses of large-scale wildfire datasets. As wildfire databases become larger and cover longer time periods, the consideration of aggregation methods and the MAUP will become even more significant.

2. Methods & Data

The central aim of our research was to assess the effects of different aggregation schemes on wildfire analyses. Four data sources were used. Wildfire point data during 1981-2016 were downloaded from the U.S. Federal Wildland Fire Occurrence Database (United States Department of Interior, 2018). The U.S. Environmental Protection Agency (U.S. EPA) provided different levels of ecoregion polygon data, including Level I, II, and III ecoregions for North America (U.S. EPA, 2016) and Level IV ecoregions for the contiguous U.S.(U.S. EPA, 2016b).Annual climate data (Maximum vapor-pressure deficit (VPD_{max}), average temperature (T_{mean}), and total precipitation (PPT_{total})) rasters at 4km resolution during 1981-2016 were downloaded from the Parameter-Elevation Regressions on Independent Slopes Model (PRISM) (Di Luzio *et al.*, 2008).

The federal agencies that provided the wildfire data manage almost half of the land in the western U.S. (Vincent *et al.*, 2017), so the study area was limited to the Western U.S. to mitigate sampling errors due to the lack of federally managed land (and

thus wildfire data) in more eastern states. State data could supplement federal data in the Eastern U.S., but combining state and federal data is challenging in terms of the differing quality and reporting formats used across agencies. Via Environmental Systems Research Institute (ESRI) ArcMap, all the data were set to the world cylindrical equal area projection. The data were restricted to those from Arizona, California, Colorado, Idaho, Montana, Nevada, New Mexico, Oregon, Utah, Washington, and Wyoming, where the vast majority of wildfires occur in the lower 48 states.

The study area includes 100 Level I polygons, 103 Level II polygons, 155 Level III polygons, 3,259 Level IV polygons, and 529,933. Data on small wildfires (<1 acre) are often incomplete or inaccurate because small wildfires may go undetected and/or unreported. Therefore, wildfires which burned <1 acre were excluded, leaving 143,762 unevenly distributed wildfire points (Figure 1). Islands were removed from the ecoregion polygons, leaving44 Level I polygons, 47 Level II polygons, 85 Level III polygons, and 3,188 Level IV polygons (Figure 2). Note the high degree of similarity between Level I and Level II ecoregions, and the extremely high number of polygons in the Level IV ecoregions.

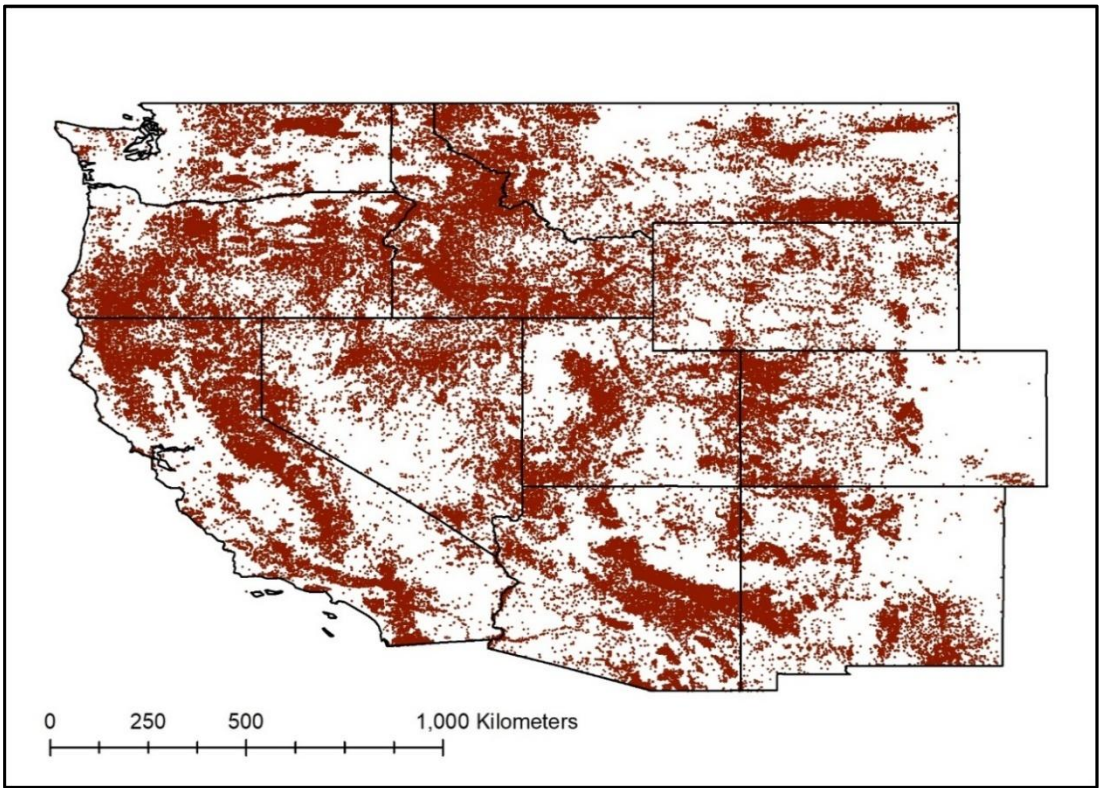

Figure 1. The distribution of wildfires which burned more than 1 acre 1981-2016 in the western U.S. Derived from the U.S. Federal Wildland Fire Occurrence Database

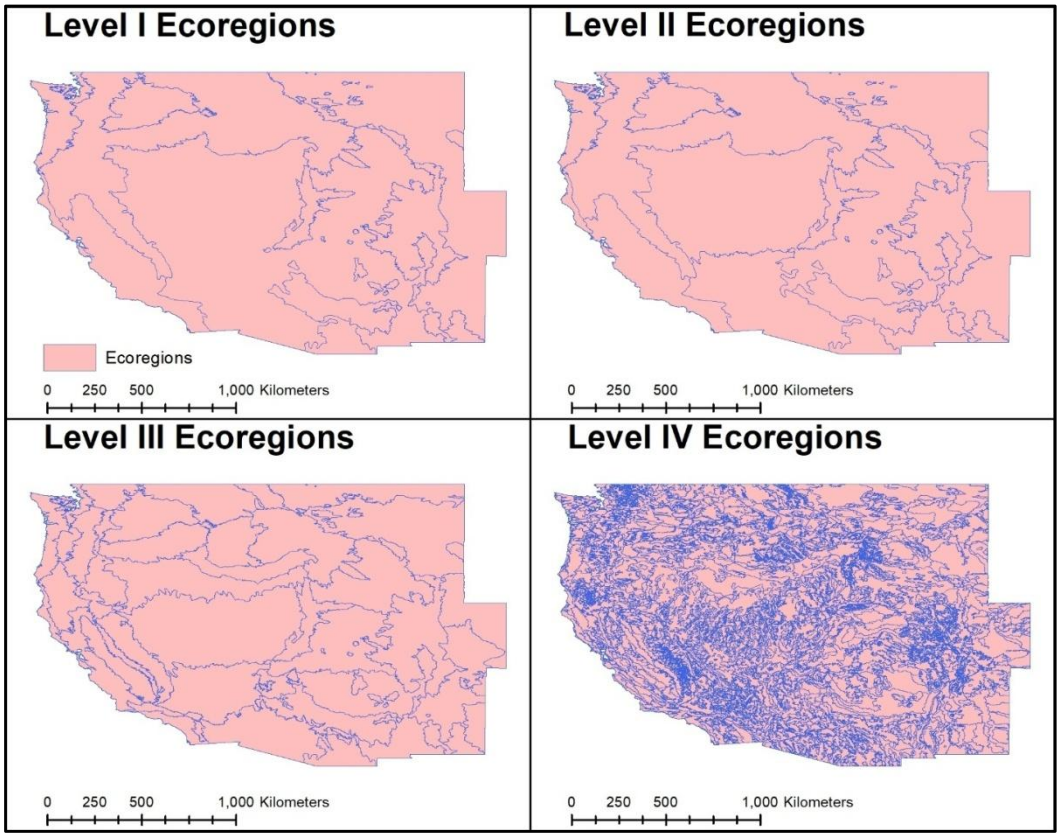

Figure 2. The ecoregion polygons in the western U.S. Note that the Level I and Level II ecoregions have very similar polygons, while there is an increase in detail between the Level II and the Level III ecoregions and a huge increase in the number of polygons between the Level III and Level IV polygons.

Fishnet polygons were generated for scale and shape comparisons. Square, triangular, and hexagonal fishnets were created over the western United States with areas of 16km^2, 64km^2, 256km^2, 1,024km^2, 4,096km^2, 16,384km^2, and 65,536km^2(Figure 3-5).

The wildfire and climate data were then aggregated to each of the fishnet and ecoregion polygons. The following wildfire variables were calculated and added to the polygon files: the total number of fires within each polygon, the total acres burned within each polygon, and the median fire size within each polygon. For the ecoregion polygons, the total area burned was normalized to the area of each polygon. The following climate variables were then calculated within each polygon and added to the polygon files: the average of the VPD_{max} values, the average of the T_{mean} values, and the average of the PPT_{total} values.

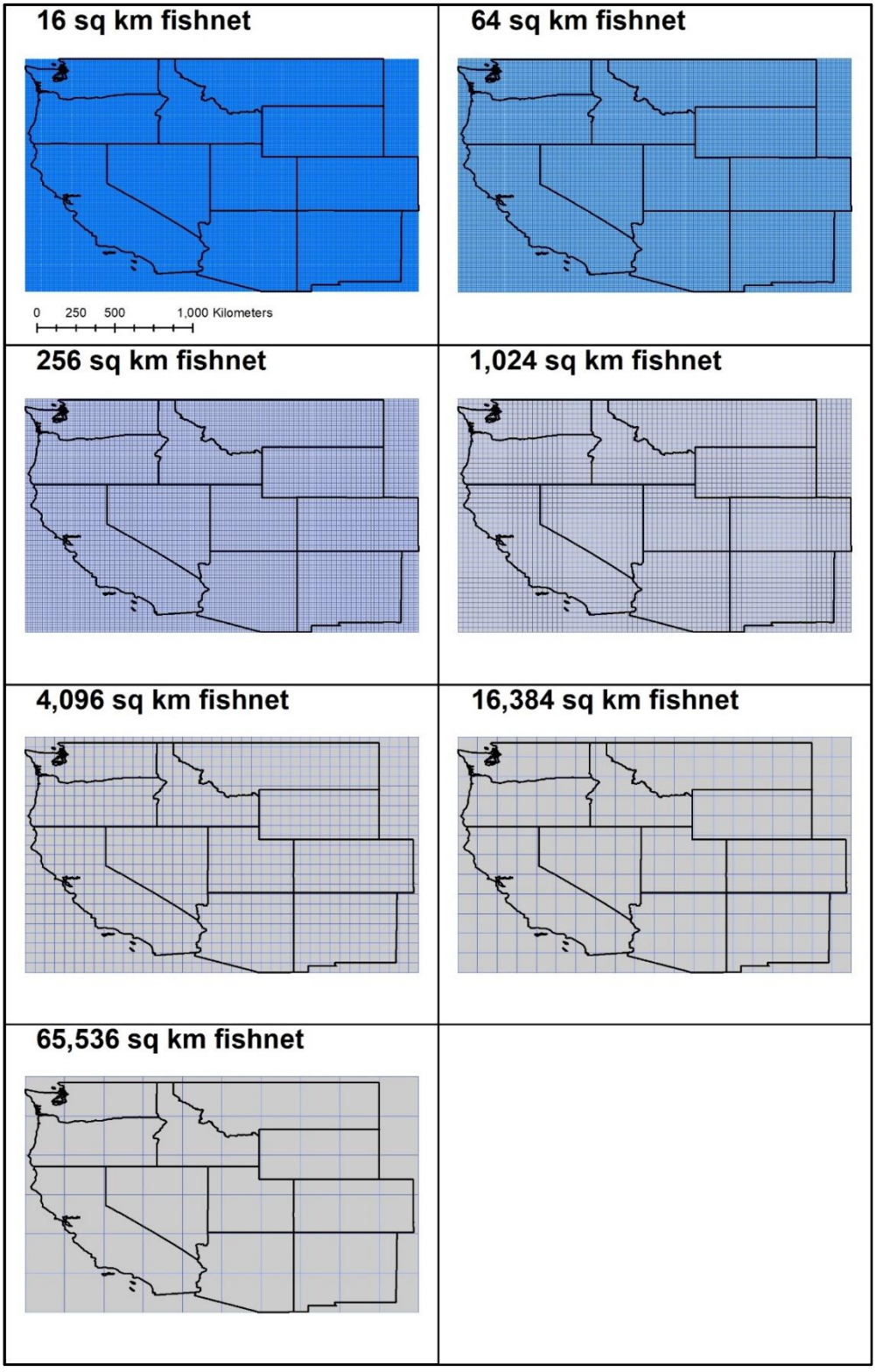

Figure 3. The square fishnet polygons used in this study. Note that the extent remains constant across all fishnets, while the size and location of each square differs.

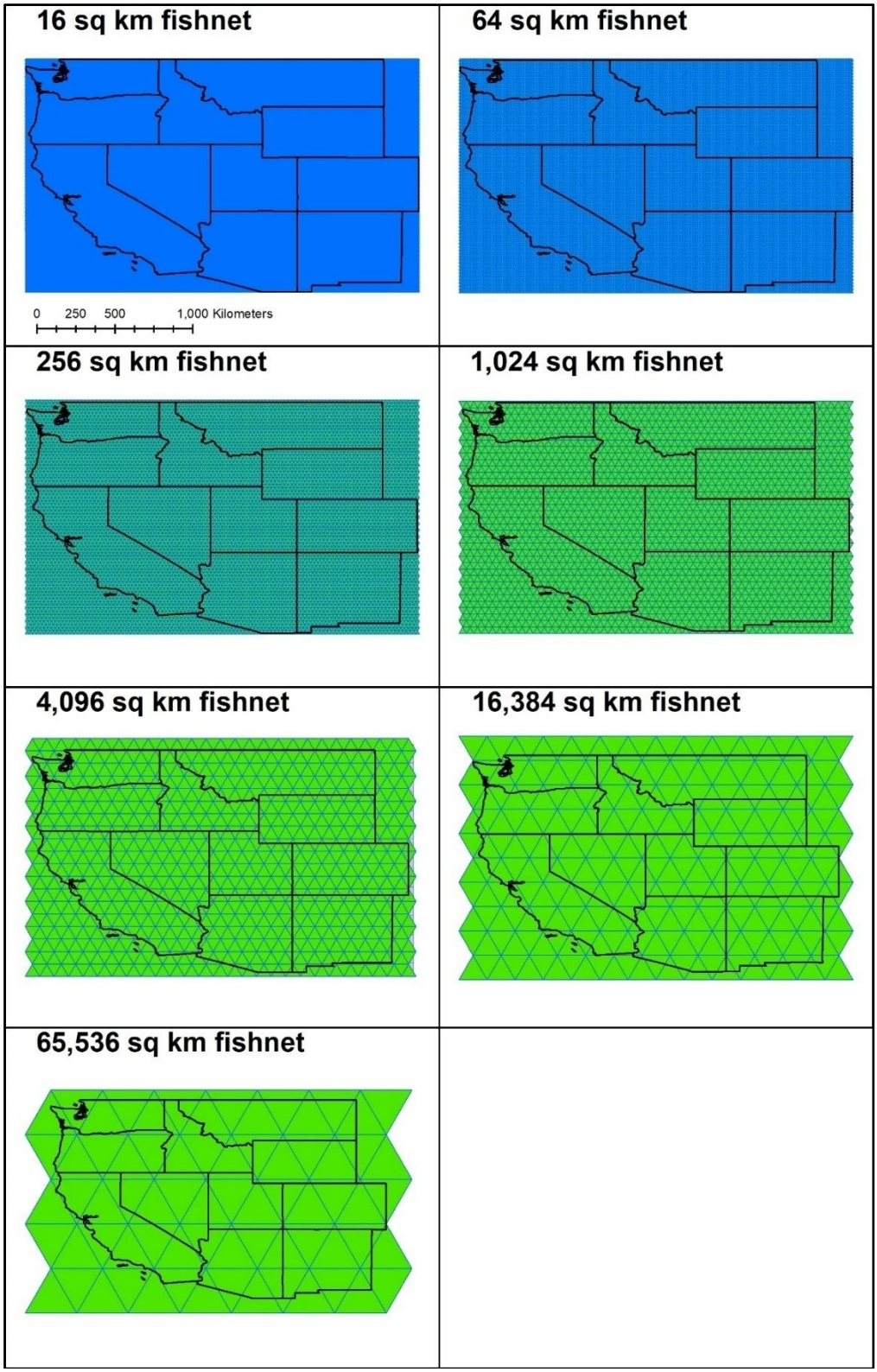

Figure 4. The triangular fishnet polygons used in this study. Note that the extent varies across the fishnets, and the size and location of each triangle differs

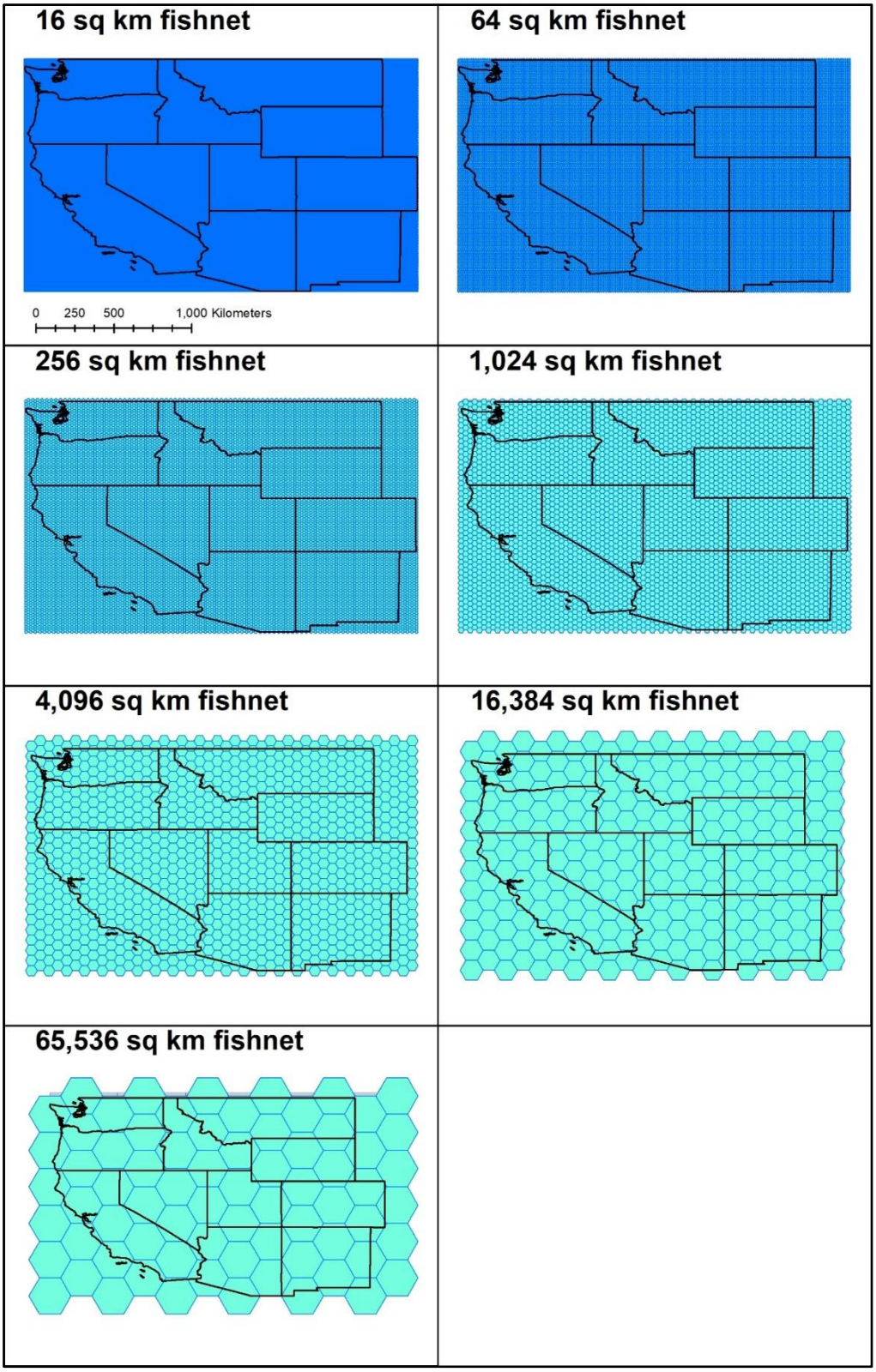

Figure 5. The hexagonal fishnet polygons used in this study.Note that the extent varies across the fishnets, and the size and location of each hexagon differs

Queen-style contiguity row-standardized spatial weights were generated for each set of polygons in R-Studio. These weights are stored in a matrix, and they define which polygons are considered neighbors for later testing. Global Moran's Index (commonly known as Moran's I) (Moran, 1950) values were calculated for the total area burned in each set of polygons. Moran's I measures autocorrelation, or the correlation of a variable with itself through space (Sokal & Oden, 1978; Legendre, 1993; Getis & Ord, 1995). Spatial autocorrelation can be positive (when similar values occur near one another) or negative (when dissimilar values occur near one another). In this case, Moran's I measures to what extent wildfires were likely to burn adjacent polygons. Moran's I is based on cross-products of the deviations from the mean, and is calculated for *n* observations on a variable *x* at locations *i*, *j* as:

$$I = \frac{n}{S_0} \frac{\sum_i \sum_j w_{ij}(x_i - \bar{x})(x_j - \bar{x})}{\sum_i (x_i - \bar{x})^2}$$

where $\bar{x}$ is the mean of the *x* variable, w_{ij} are the elements of the weight matrix, and S_0 is the sum of the elements of the weight matrix: $S_0 = \sum_i \sum_j w_{ij}$ .Moran's I value varies from -1 (essentially perfect negative autocorrelation) to +1 (essentially perfect positive autocorrelation).

A standard ordinary least squares regression (OLS) model was applied to each set of polygons with total area burned as the dependent variable, and VPD_{max}, T_{mean}, and PPT_{total} as independent variables. OLS models take the form:

$$y_i = \beta_1 x_{1i} + \beta_2 x_{2i} + \cdots + \beta_n x_{ni} + \varepsilon_i$$

where y_i is the dependent variable, x_{ji} (j from 1 to n) are the set of independent variables, and ε_i is the residual, all at location i. To address the spatial autocorrelation in the regression, either the spatial lag (Anselin, 2003, 2013) or spatial error model (Bartels & Hordijk, 1977; Brandsma & Ketellapper, 1979; Anselin, 2013) can be used to perform the regression analysis.

OLS models are best suited to data where there are no influences from any spatial neighbors, spatial lag models are best suited to data where the dependent variable is influenced by spatial neighbors, and spatial error models are best suited to data where the residuals are influenced by spatial neighbors (Baller et al., 2001). Further, the spatial lag model is best used in cases where a substantive spatial process is of interest, while spatial error models are more appropriate where variables have likely been omitted, or where there is a mismatch between the data scale and spatial process scale.

Moran's Index, Lagrange multiplier (LM), and robust Lagrange multiplier (RLM) (Breusch & Pagan, 1980; Anselin, 1988) tests were both performed on the OLS residuals. Using an 'Anselin Style' model selection strategy (Anselin & Rey, 1991; Anselin, 2005), the appropriate model was selected (Figure 6).

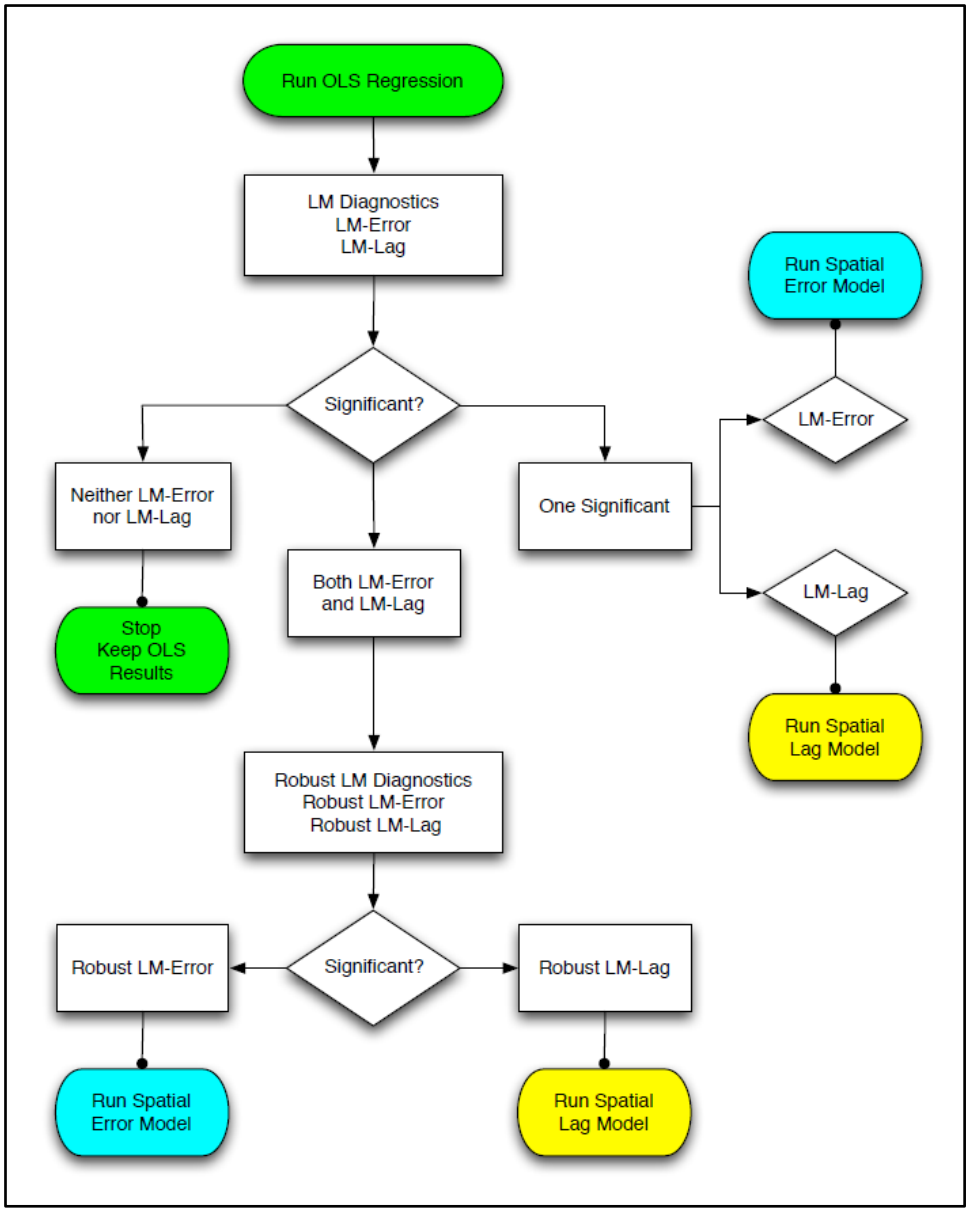

Figure 6. The Anselin method for selecting the appropriate regression model. If both lag and error tests are significant, the test with the lower value was be used (modified from Anselin (2005)).

Spatio-temporal analyses were run in ESRI ArcGIS Pro. For each set of fishnets, a 'space time cube' was generated via the *Create Space Time Cube By Aggregating Points*tool (ESRI, 2019a). In this process, wildfire points are aggregated by a certain time interval, in this case one year, then aggregated and summed to the polygon which contains them. An *Emerging Hotspot Analysis* (Environmental Systems Research Institute, 2019b) was then performed on each space time cube. For the Emerging Hotspot Analysis in this study, spatial neighbors were defined by queen-style spatial contiguity, and temporal neighbors were defined as one year. This technique combines two well established statistical tests: the Getis Ord Gi* (Getis & Ord, 1992; Getis & Ord, 1995) to measure hot (dense and/or frequent occurrences) and cold (sparse and/or

infrequent occurrences)spots in space, and the Mann-Kendall trend test (Mann, 1945; Kendall & Gibbons, 1990) to measure trends through time. This analysis produces one of seventeen classifications for each polygon (Environmental Systems Research Institute, 2019b).

3. Results

Three pairs of ecoregion and fishnet polygons were of comparable average size: 1) The Level IV ecoregions and the #4 fishnets (differing in area by 6.3%), 2) the Level II ecoregions and the #7 fishnets(differing in area by 0.3%), and 3) the Level I ecoregions and the #7 fishnets by (differing in area by 6.1%) (Table 1).

Table 1. Selected characteristics of different aggregation schemes

Aggregation scheme	Average polygon area (km^2)	Number of polygons	Average area burned per polygon (acres)	Average number of wildfires per polygon
Level I Ecoregions	*69,775*	*44*	*2.42×10^6*	*3,266.3*
Level II Ecoregions	*65,321*	*47*	*2.27×10^6*	*3,057.9*
Level III Ecoregions	*36,119*	*85*	*1.25×10^6*	*1,690.8*
Level IV Ecoregions	*963*	*3,188*	*3.34×10^4*	*45.1*
Square fishnet 1	*16*	*236,368*	*1.90×10^3*	*0.6*
Square fishnet 2	*64*	*59,408*	*4.05×10^3*	*2.4*
Square fishnet 3	*256*	*14,852*	*1.13×10^4*	*9.7*
Square fishnet 4	*1,024*	*3,713*	*3.78×10^4*	*38.7*
Square fishnet 5	*4,096*	*960*	*1.37×10^5*	*149.8*
Square fishnet 6	*16,384*	*240*	*5.07×10^5*	*599.0*
Square fishnet 7	*65,536*	*60*	*1.90×10^6*	*2,396.0*
Triangular fishnet 1	*16*	*237,405*	*1.890×10^3*	*0.6*
Triangular fishnet 2	*64*	*59,631*	*4.036×10^3*	*2.4*
Triangular fishnet 3	*256*	*15048*	*1.121×10^4*	*9.6*
Triangular fishnet 4	*1,024*	*3,780*	*3.743×10^4*	*38.0*
Triangular fishnet 5	*4,096*	*1,007*	*1.345×10^5*	*142.8*
Triangular fishnet 6	*16,384*	*270*	*4.672×10^5*	*532.5*
Triangular fishnet 7	*65,536*	*70*	*1.718×10^6*	*2,053.7*
Hexagonal fishnet 1	*16*	*23,7320*	*1.900×10^3*	*0.6*
Hexagonal fishnet 2	*64*	*59,500*	*4.061×10^3*	*2.4*
Hexagonal fishnet 3	*256*	*15,048*	*1.129×10^4*	*9.6*
Hexagonal fishnet 4	*1,024*	*3,784*	*3.780×10^4*	*38.0*
Hexagonal fishnet 5	*4,096*	*1,012*	*1.350×10^5*	*142.1*
Hexagonal fishnet 6	*16,384*	*264*	*4.954×10^5*	*544.6*
Hexagonal fishnet 7	*65,536*	*72*	*1.746×10^6*	*1,996.7*

Keeping area relatively constant, polygon shape can affect statistical findings. The influence of polygon shape can be examined by comparing the number of wildfires and the total area burned across the three sets of similarly-sized polygons. The Level IV ecoregions had 15% more wildfires per polygon on average than the #4 fishnets, while the Level II ecoregions had 30% more wildfires than the #7 fishnets and the Level I ecoregions had 34% more wildfires than the #7 fishnets. The Level IV ecoregions had a 13% larger area burned on average than the #4 fishnet, the Level II ecoregions had a 21%larger area burned than the #4 fishnets, and the Level I ecoregions had a 26% larger area burned than the #4 fishnets.

In these three comparisons, the ecoregions had fewer polygons than the fishnets, indicating that the average area was dragged down by relatively few very small

polygons. The #4 fishnets had an average of 18% more polygons than the Level IV ecoregions (3,759 versus 3,188), the #7 fishnets had an average of 43% more polygons than the Level II ecoregions (67 versus 47), and an average 53% more polygons than the Level I ecoregions (67 versus 44).

Testing the autocorrelation of the total area burned revealed differences across the aggregation schemes. Using the ecoregions, aggregation scale altered significance of autocorrelation in the total area burned. The Level III and Level IV ecoregions had significant autocorrelation at 0.05 and 0.01 level respectively (Table 2). However, the significance of the autocorrelation was not proportional to the average polygon area, as the Level I ecoregions had larger Moran's I value than the Level II ecoregions.

For all of the fishnet polygons, aggregation scale altered the magnitude of autocorrelation in the total area burned and its significance. Every scale had significant ($p < 0.01$) autocorrelation (Table 2), but different Z-scores (Figure 7). The Z-scores of the fishnet polygons form right-skewed inverted parabolas that peak between 256 km^2 and 1,024 km^2, while the Level III and IV ecoregions both have Z-scores between 2 and 4.

Table 2. Moran's I test results for the total area burned

Aggregation scheme	Level | Area (km^2)		Global Moran's I p-value	Global Moran's I Z-score	Global Moran's I
Ecoregions	I	*69,775*	*0.2063*	*0.82*	*0.07*
	II	*65,321*	*0.3348*	*0.43*	*0.03*
	III	*36,119*	*0.0121***	*2.26*	*0.18*
	IV	*963*	*0.0051**	*2.57*	*0.03*
Square fishnet	*16*		*2.20×10^{-16}**	*18.84*	*0.02*
	64		*2.20×10^{-16}**	*24.04*	*0.05*
	256		*2.20×10^{-16}**	*31.16*	*0.12*
	1,024		*2.20×10^{-16}**	*31.99*	*0.26*
	4,096		*2.20×10^{-16}**	*22.35*	*0.37*
	16,384		*2.20×10^{-16}**	*13.23*	*0.44*
	65,536		*1.06×10^{-9}**	*5.99*	*0.39*
Triangular fishnet	*16*		*2.20×10^{-16}**	*26.66*	*0.02*
	64		*2.20×10^{-16}**	*28.98*	*0.05*
	256		*2.20×10^{-16}**	*35.16*	*0.11*
	1,024		*2.20×10^{-16}**	*33.31*	*0.22*
	4,096		*2.20×10^{-16}**	*22.88*	*0.30*
	16,384		*2.20×10^{-16}**	*15.38*	*0.40*
	65,536		*1.19×10^{-12}**	*7.01*	*0.34*
Hexagonal fishnet	*16*		*2.20×10^{-16}**	*20.33*	*0.02*
	64		*2.20×10^{-16}**	*22.38*	*0.05*
	256		*2.20×10^{-16}**	*29.57*	*0.14*
	1,024		*2.20×10^{-16}**	*27.88*	*0.26*
	4,096		*2.20×10^{-16}**	*20.48*	*0.38*
	16,384		*2.20×10^{-16}**	*11.99*	*0.44*
	65,536		*9.07×10^{-11}**	*6.38*	*0.44*

* p-value< 0.01
** p-value< 0.05

Keeping area constant, the Z-scores of the Moran's I test varied across the three different fishnet shapes (Figure 7). The triangular fishnet (3 neighbors per polygon) had the highest Z-scores, while the hexagonal fishnet (6 neighbors per polygon) had the lowest Z-scores except at the extreme ends of the size ranges (16km^2 and 65,536km^2). The triangular and hexagonal fishnets peaked at 256km^2, while the square fishnet peaked at 1,024km^2.

Moran's I values varied by polygon size, with smaller areas corresponding to lower values, and larger areas corresponding to higher values (Figure 8). The Moran's Ivalues of the Level III ecoregion data were much smaller than the indexes of the corresponding fishnet data with similar average polygon areas. The shape of the polygons changed the significance of the autocorrelation.

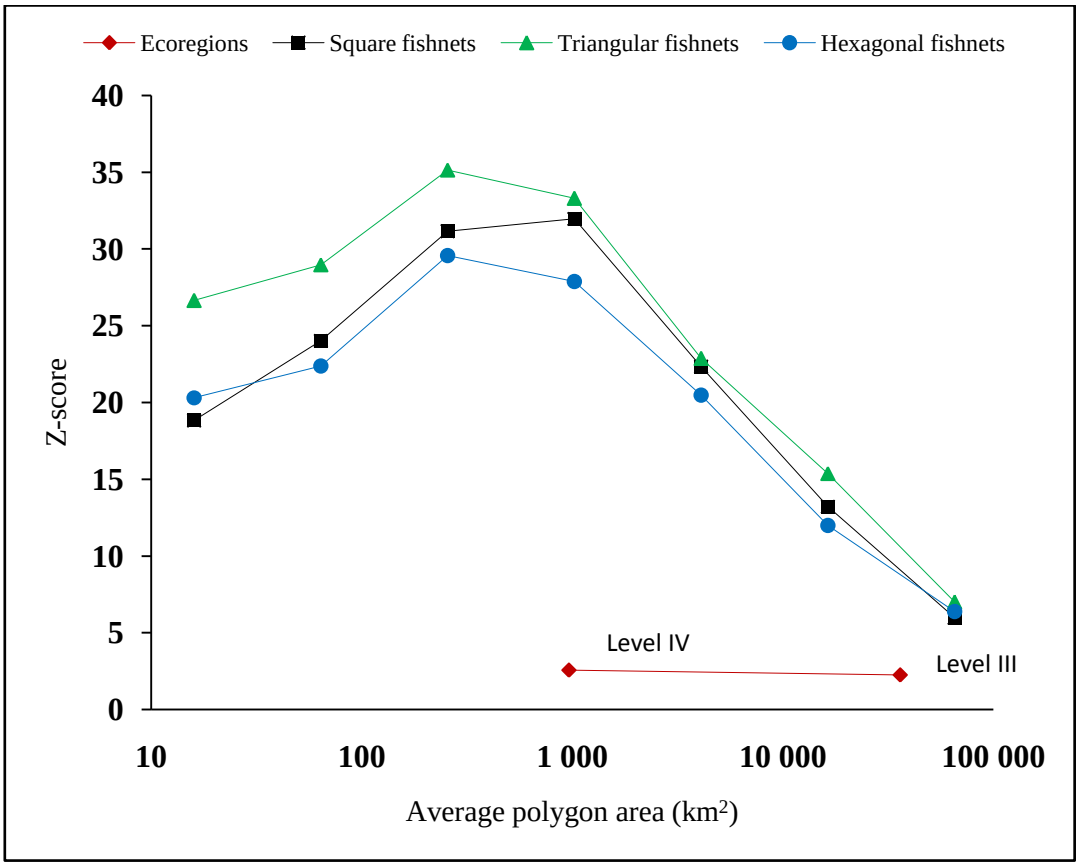

Figure 7. Moran's I Z-scores for the total area burned by aggregation scheme. Note the log scale on the x-axis (average polygon area).

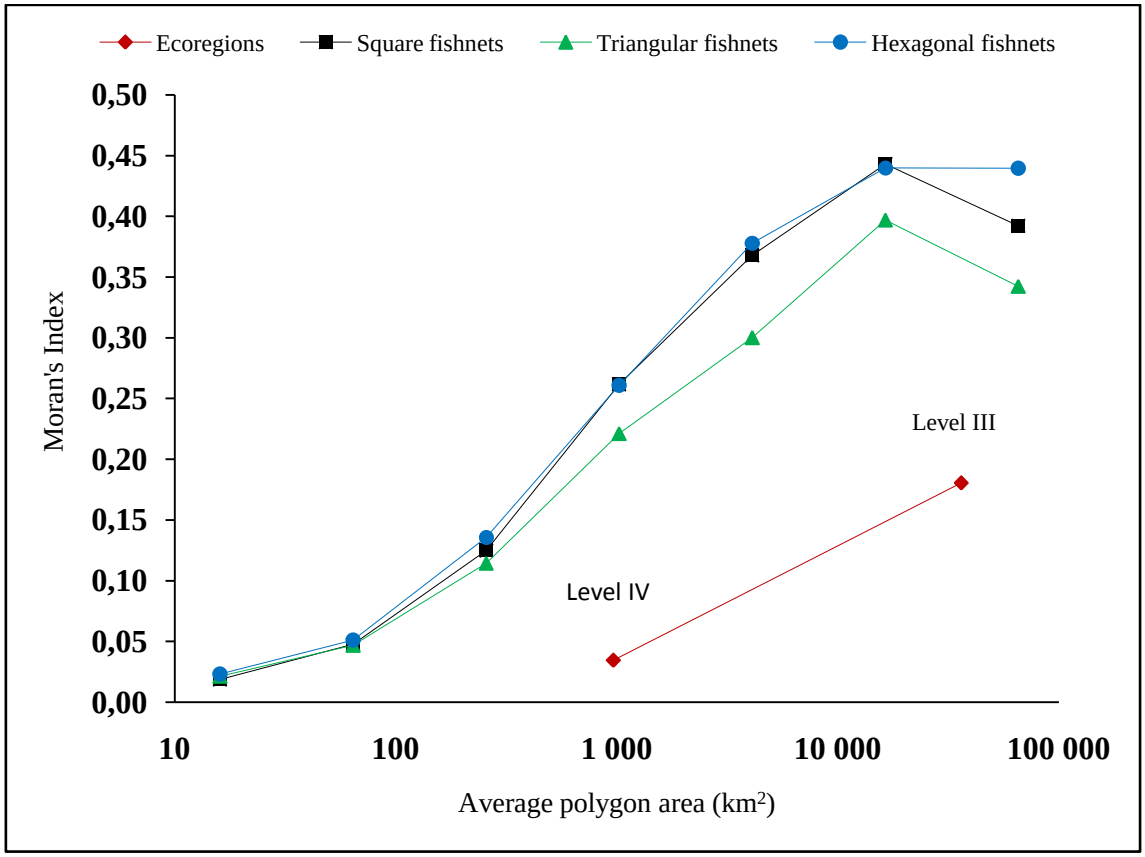

Figure 8. Moran's Index values for the autocorrelation in the total area burned by aggregation scheme. Note the log scale on the x-axis (average polygon area)

The autocorrelation in the area burned is reflected in the residuals of the OLS. The spatial autocorrelations in the residuals generated from the OLS model are shown in Table 3. Of the four ecoregions levels, again the Level III and Level IV ecoregions had significant autocorrelation among the residuals, indicating the underlying autocorrelation (Table 3). For all of the fishnet polygons, aggregation scale altered the magnitude of autocorrelation in the total area burned and its significance. Every scale had significant ($p < 0.01$) autocorrelation (Table 3), but different Z-scores (Figure 9). Keeping area constant, the Z-scores of the Moran's I test varied across the three different fishnet shapes (Figure 9). The triangular fishnet had the highest Z-scores, while the hexagonal fishnet had the lowest Z-scores except at 16km^2 where the square fishnet had the lowest Z-score. The triangular and hexagonal fishnets again both peaked at 256km^2, while the square fishnet peaked at 1,024km^2.

Moran's Index varied by polygon size, with smaller areas corresponding to lower values, and larger areas corresponding to higher values (Figure 10). The Moran's Index of the Level III ecoregion data was again much lower than the indexes of the fishnet data with similar average polygon sizes.

Table 3. Moran's I test results for OLS residuals

Aggregation scheme	Level / Area (km^2)		Global Moran's I p-value of OLS residuals	Global Moran's I Z-score of OLS residuals	Global Moran's Index of OLS residuals
Ecoregions	I	*69,775*	*0.4180*	*0.21*	*-0.03*
	II	*65,321*	*0.5665*	*-0.17*	*-0.07*
	III	*36,119*	*0.0324***	*1.85*	*0.13*
	IV	*963*	*0.0127***	*2.24*	*0.03*
Square fishnet	*16*		*2.20×10^{-16}**	*17.6*	*0.018*
	64		*2.20×10^{-16}**	*22.4*	*0.046*
	256		*2.20×10^{-16}**	*29.2*	*0.120*
	1,024		*2.20×10^{-16}**	*30.4*	*0.253*
	4,096		*2.20×10^{-16}**	*22.1*	*0.362*
	16,384		*2.20×10^{-16}**	*13.5*	*0.433*
	65,536		*1.20×10^{-12}**	*7.0*	*0.402*
Triangular fishnet	*16*		*2.20×10^{-16}**	*25.1*	*0.021*
	64		*2.20×10^{-16}**	*27.0*	*0.045*
	256		*2.20×10^{-16}**	*32.8*	*0.110*
	1,024		*2.20×10^{-16}**	*31.7*	*0.213*
	4,096		*2.20×10^{-16}**	*22.3*	*0.290*
	16,384		*2.20×10^{-16}**	*15.7*	*0.386*
	65,536		*4.16×10^{-16}**	*8.0*	*0.335*
Hexagonal fishnet	*16*		*2.20×10^{-16}**	*19.2*	*0.023*
	64		*2.20×10^{-16}**	*20.9*	*0.050*
	256		*2.20×10^{-16}**	*27.7*	*0.131*
	1,024		*2.20×10^{-16}**	*26.6*	*0.252*
	4,096		*2.20×10^{-16}**	*19.7*	*0.364*
	16,384		*2.20×10^{-16}**	*11.9*	*0.424*
	65,536		*1.33×10^{-11}**	*6.7*	*0.421*

* p-value< 0.01
** p-value< 0.05

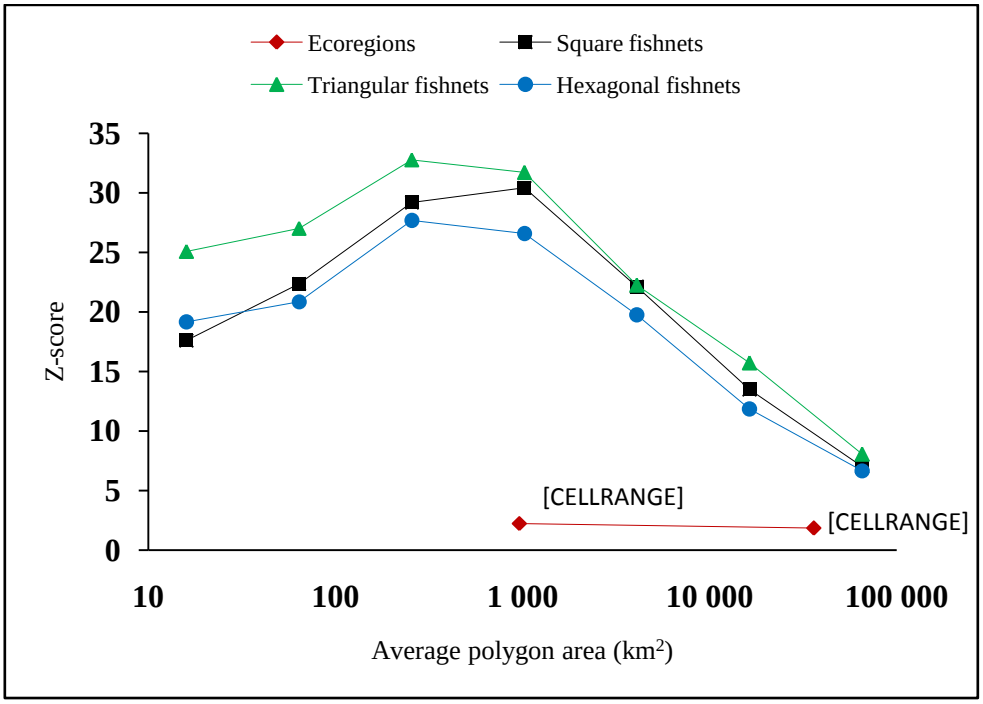

Figure 9. Moran's I Z-scores for the OLS residuals by aggregation scheme. Note the log scale on the x-axis (average polygon area)

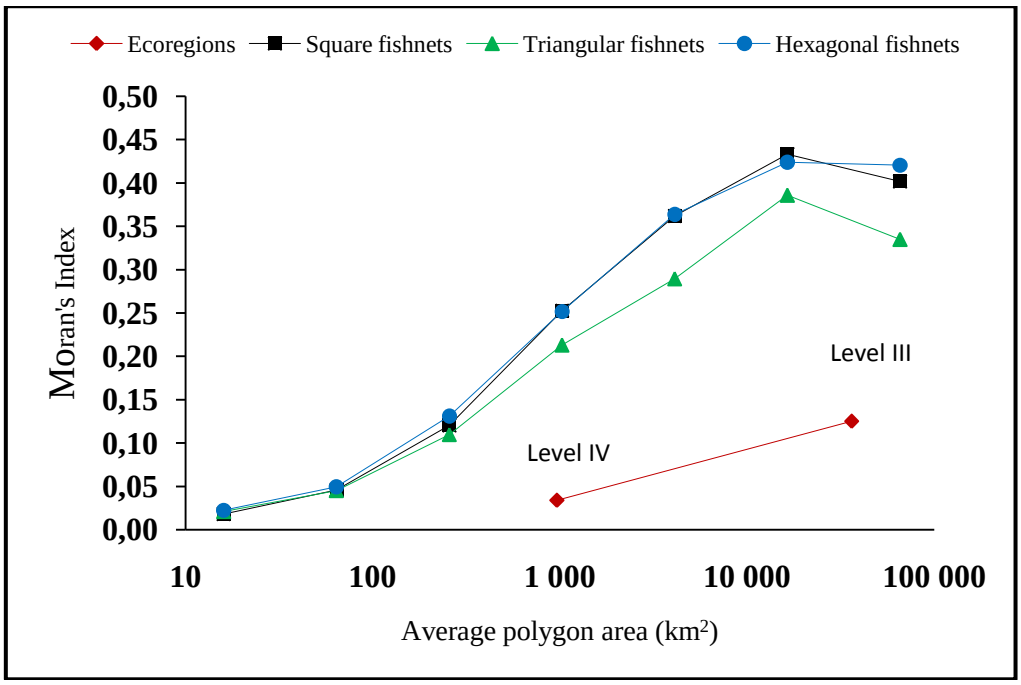

Figure 10. Moran's Index values for the autocorrelation in the OLS residuals by aggregation scheme. Note the log scale on the x-axis (average polygon area).

The choice of aggregation scheme affected which spatial model should be used according to the Anselin selection method (Table 4). The OLS LM/RLM testing found that of the twenty-five aggregation schemes, ten were best suited by an OLS model, six by a spatial lag model, and nine to a spatial error model (Table 4). Scale had a larger effect than shape: within fishnet styles, the optimal model varied unpredictably with polygon area, while across fishnet styles the optimal model was consistent at except at 64km^2 (Square: spatial error, Triangular: OLS, Hexagonal: Spatial lag).

Table 4. Lagrange Multiplier test results and corresponding model according to the Anselin method

Aggregation scheme	Level | Area (km^2)		LM error test	LM lag test	RLM error test	RLM lag test	Best model by Anselin method
Ecoregions	I	*69,775*	8.55×10^{-1}	9.56×10^{-1}	2.77×10^{-1}	2.83×10^{-1}	OLS
	II	*65,321*	6.17×10^{-1}	8.87×10^{-1}	5.36×10^{-3}*	6.09×10^{-3}*	OLS
	III	*36,119*	1.74×10^{-1}	9.20×10^{-2}	6.11×10^{-2}	3.40×10^{-2}**	OLS
	IV	*963*	3.07×10^{-2}**	3.11×10^{-2}**	7.96×10^{-1}	8.35×10^{-1}	Error
Square fishnet	*16*		2.20×10^{-16}*	2.20×10^{-16}*	2.33×10^{-5}*	6.81×10^{-6}*	Spatial Lag
	64		2.20×10^{-16}*	2.20×10^{-16}*	1.91×10^{-2}**	8.37×10^{-3}**	Spatial error
	256		2.20×10^{-16}*	2.20×10^{-16}*	8.30×10^{-1}	2.60×10^{-1}	OLS
	1,024		2.20×10^{-16}*	2.20×10^{-16}*	5.76×10^{-2}	8.87×10^{-1}	OLS
	4,096		2.20×10^{-16}*	2.20×10^{-16}*	1.17×10^{-4}*	2.13×10^{-1}	Spatial error
	16,384		2.20×10^{-16}*	2.20×10^{-16}*	2.75×10^{-2}**	9.42×10^{-1}	Spatial error
	65,536		5.06×10^{-8}*	1.96×10^{-7}*	8.19×10^{-2}	5.25×10^{-1}	OLS
Triangular fishnet	*16*		2.20×10^{-16}*	2.20×10^{-16}*	3.22×10^{-10}	1.83×10^{-11}*	Spatial Lag
	64		2.20×10^{-16}*	2.20×10^{-16}*	3.49×10^{-1}	1.60×10^{-1}	OLS
	256		2.20×10^{-16}*	2.20×10^{-16}*	1.78×10^{-1}	9.49×10^{-1}	OLS
	1,024		2.20×10^{-16}*	2.20×10^{-16}*	1.81×10^{-3}*	6.49×10^{-1}	Spatial Error
	4,096		2.20×10^{-16}*	2.20×10^{-16}*	6.24×10^{-4}*	6.87×10^{-1}	Spatial Error
	16,384		2.20×10^{-16}*	2.20×10^{-16}*	1.39×10^{-2}**	9.93×10^{-1}	Spatial Error
	65,536		2.77×10^{-9}	1.70×10^{-8}	5.82×10^{-2}	8.11×10^{-1}	OLS
Hexagonal fishnet	*16*		2.20×10^{-16}*	2.20×10^{-16}*	4.71×10^{-8}*	1.12×10^{-8}*	Spatial Lag
	64		2.20×10^{-16}*	2.20×10^{-16}*	8.25×10^{-3}*	4.22×10^{-3}*	Spatial Lag
	256		2.20×10^{-16}*	2.20×10^{-16}*	2.37×10^{-1}	5.72×10^{-2}	OLS
	1,024		2.20×10^{-16}*	2.20×10^{-16}*	1.31×10^{-2}**	3.26×10^{-1}	Spatial Error
	4,096		2.20×10^{-16}*	2.20×10^{-16}*	1.27×10^{-2}**	8.77×10^{-1}	Spatial Error
	16,384		2.20×10^{-16}*	2.20×10^{-16}*	8.39×10^{-3}*	9.24×10^{-1}	Spatial Error
	65,536		3.55×10^{-8}	9.28×10^{-8}	1.62×10^{-1}	7.65×10^{-1}	OLS

* p-value< 0.01
** p-value< 0.05

The choice of aggregation scheme also affected the results from the Emerging Hotspot Analysis. The analysis only detected four classifications: 1) no pattern, 2) sporadic hot spot, 3) consecutive hot spot, and 4) new hotspot (Table 5). In every case, the vast majority of polygons had no pattern (Table 5). Sporadic hotspots were the second most common classification except for the scales of 16km^2 and 64km^2, where consecutive hotspots were second most common, and new hotspots were the least common of all the detected classifications (Tables 5).

Polygon shape further affected the classification results. The triangular fishnets had the most sporadic hotspots, while the hexagonal fishnets had the fewest (Table 5). Consecutive and new hot spots did not demonstrate the same pattern (Table 5).Intra-scale classification variation generally increased with polygon size from 0.2% at 16km^2 to 9% at 65,536km^2.

Table 5. Results of the emerging hotspot analysis. Bold indicates the largest normalized fraction of each hotspot type

Area (km^2)	Fishnet shape	No Pattern: # - (%)	Sporadic Hot Spots: # - (%)	Consecutive Hot Spots: # - (%)	New Hot Spots: # - (%)
16	Square	*235,673- (99.71)*	*102- (0.04)*	*302- (0.13)*	*291- (0.12)*
	Hexagonal	*236,728- (99.75)*	*76- (0.03)*	*283- (0.12)*	*233- (0.10)*
	Triangular	*236,480 - (99.61)*	***182 - (0.08)***	***364 - (0.15)***	***379 - (0.16)***
% Range		*0.14*	*0.04*	*0.03*	*0.06*
64	Square	*58,967- (99.26)*	*133- (0.22)*	*184- (0.31)*	*124- (0.21)*
	Hexagonal	*59,113- (99.35)*	*89- (0.15)*	*164- (0.28)*	***134 - (0.23)***
	Triangular	*59,072- (99.06)*	***177 - (0.30)***	***250 - (0.42)***	*132- (0.22)*
% Range		*0.29*	*0.15*	*0.14*	*0.02*
256	Square	*14,601- (98.31)*	*104- (0.70)*	*96- (0.65)*	***51 - (0.34)***
	Hexagonal	*14,847- (98.66)*	*82- (0.54)*	*86- (0.57)*	*33- (0.22)*
	Triangular	*14,733- (97.91)*	***153 - (1.02)***	***123 - (0.82)***	*39- (0.26)*
% Range		*0.76*	*0.47*	*0.25*	*0.12*
1,024	Square	*3,605- (97.09)*	*54- (1.45)*	*36- (0.97)*	***18 - (0.48)***
	Hexagonal	*3,683- (97.33)*	*49- (1.29)*	***43 - (1.14)***	*9- (0.24)*
	Triangular	*3,653- (96.64)*	***73 - (1.93)***	*36- (0.95)*	***18 - (0.48)***
% Range		*0.69*	*0.64*	*0.18*	*0.25*
4,096	Square	*911- (94.90)*	*38- (3.96)*	*8 - (0.83)*	*3 - (0.31)*
	Hexagonal	*962- (95.06)*	*36- (3.56)*	***10 - (0.99)***	***4 - (0.40)***
	Triangular	*948- (94.14)*	***51 - (5.06)***	*8 - (0.79)*	*0 - (0.00)*
% Range		*0.92*	*1.51*	*0.19*	*0.40*
16,384	Square	*218 - (90.83)*	***16 - (6.67)***	***5 - (2.08)***	*1 - (0.42)*
	Hexagonal	*243 - (92.05)*	*16 - (6.06)*	*5 - (1.89)*	*0 - (0.00)*
	Triangular	*245 - (90.74)*	***18 - (6.67)***	*5 - (1.85)*	***2 - (0.74)***
% Range		*1.30*	*0.61*	*0.23*	*0.74*
65,536	Square	*52- (86.67)*	*6- (10.00)*	***2 - (3.33)***	***0 - (0.00)***
	Hexagonal	*64- (88.89)*	*7- (9.72)*	*1 - (1.39)*	***0 - (0.00)***
	Triangular	*56- (80.00)*	***12 - (17.14)***	*2 - (2.86)*	***0 - (0.00)***
% Range		*8.89*	*7.42*	*1.94*	--

Aggregation scale and shape affected the spatial distribution of the results (Figure 11). The results of the 16km^2 fishnets are extremely similar (Figure 11 Row A). Differences in classifications across the polygon shapes are largely due to variations hot the hotspot polygons are grouped (e.g. the hotspots are almost entirely located in the same areas, but have slightly different shapes and thus different numbers of hotspot polygons). The results of the 64km^2 fishnets are very similar (Figure 11 Row B) with a few variations in new hotspots in eastern Oregon, northwest Wyoming, eastern Arizona, and western New Mexico.

The results of the 256km^2 fishnets have very consistent groups of hotspots, with variations in shape largely driven by the shape of the fishnets themselves (Figure 11 Row C). There are two notable exceptions: 1) a group in northern California that is a new hotspot in the square fishnet, a consistent hotspot in the hexagonal fishnet, and not a hotspot in the triangular fishnet, and 2) a group in eastern Arizona that is a new hotspot in the square fishnet, not a hotspot in the hexagonal fishnet, and a consistent hotspot in the triangular fishnet.

The results of the 1,024km^2 fishnets have similar groups of hotspots, but differ in their classifications (Figure 11 Row D). A group in northeastern Washington is composed of new hotspots in the square fishnet, but consistent hotspots in the hexagonal and triangular fishnets. Similarly, there is a group in central California that is composed of consistent hotspots in the square and hexagonal fishnets, but has some new hotspots in the triangular fishnet. Finally, there is a group in in central Oregon that is a consistent hotspot in the triangular and hexagonal fishnets, but is not a hotspot in the square fishnet.

The results of the 4,096km^2 fishnets are largely similar (Figure 11 Row E) with four exceptions: 1) a cell in south-central Washington that is a new hotspot in the square and hexagonal fishnets, but a sporadic hotspot in the triangular fishnet, 2) a group in central Oregon that is a sporadic hotspot in the square fishnet, a new hotspot in the hexagonal fishnet, and a consistent hotspot in the triangular fishnet, 3) a group along the California-Nevada border that is composed of all three types of hotspots in the square fishnet, sporadic and new hotspots in the hexagonal fishnet, and is not a hotspot in the triangular fishnet, and 4) a group in northern Idaho composed of sporadic and consistent hotspots in the square fishnet, all three types of hotspots in the hexagonal fishnet, and only sporadic hotspots in the triangular fishnet.

The results of the16,384km^2 fishnets are mostly similar (Figure 11 Row F) with two exceptions: 1) a group of new hotspots in northeast Washington that is only present in the triangular fishnet, and 2) a group along the Washington-Oregon border that is composed of a new and sporadic hotspot in the square fishnet, but only sporadic hotspots in the hexagonal and triangular fishnets.

The results of the 65,536km^2 fishnets have very similar distributions (Figure 11 Row G): sporadic hotspots cover the inland Pacific Northwest, with a patch of consecutive hotspots in western Washington.

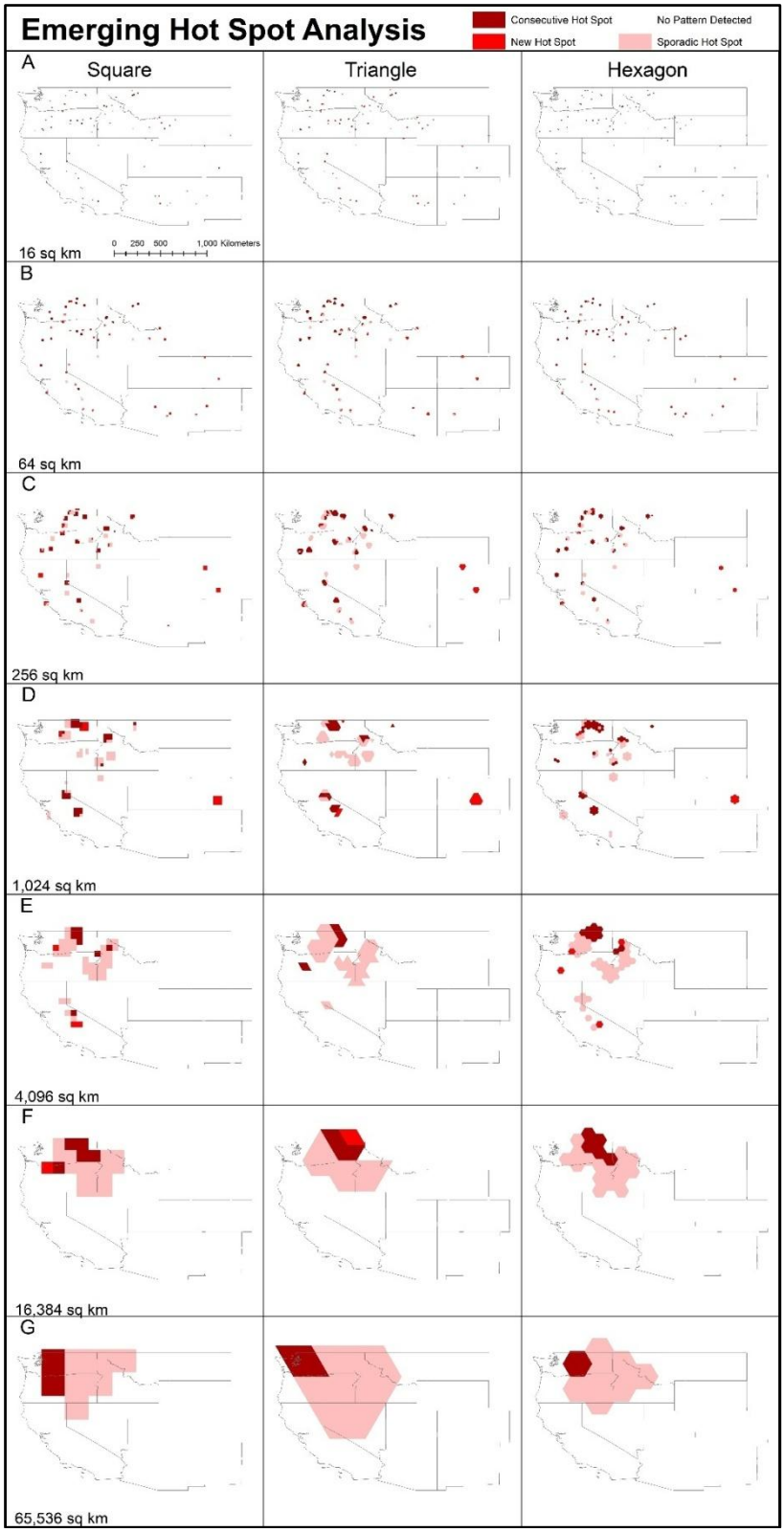

Figure 11. Spatial distributions of results from the emerging hot spot analysis by aggregation schemeA) 16km^{2}fishnets, B) 64km^{2}fishnets, C) 256km^{2}fishnets, D) 1,024km^{2}fishnets, E) 4,096km^{2}fishnets, F) 16,384km^{2}fishnets, G) 65,536km^{2}fishnets.Note the obvious variability down each column (scale problem) as well as the variability across the rows (zone problem).

4. Discussion

Our results demonstrate the effects that the MAUP can have on wildfire analyses that rely on point aggregation. This study was focused on quantifying some of the variability in results that arise from differing aggregation polygon sizes and shapes and not on perfectly modeling wildfire occurrence, patterns, or correlations with other variables (a great deal of this work already exists in the literature). For example, the OLS testing revealed that there were likely variables missing from the regression (i.e. the model is mis-specified). However, because all of the models were equally mis-specified, inter-model comparisons were justified.

The variability in burned area autocorrelation indicated the importance of the MAUP to future wildfire studies. Mitigating or correcting for the effects of autocorrelation is of primary importance in geospatial analyses, as demonstrated by the development of model selection strategies like Anselin (1991). However, the Moran's I results demonstrated that the level of autocorrelation in the total area burned was not consistent across polygon shape or scale. The Level III and IV ecoregions had significant autocorrelation in the total area burned. Without testing the autocorrelation across scales, it would be impossible to predict the results because there is nothing intrinsic to the smaller ecoregions that should promote greater autocorrelation in those polygons versus the other defined ecoregions. Further, while all of the fishnet polygons had significant autocorrelation to varying degrees, this study was limited to three geometries across seven scales. Studies which aggregate data to fishnet or ecoregion polygons should be judicious in their aggregation scale and shape, as the magnitude of the autocorrelation is variable, and may not be significant in every case, and should take the effects of autocorrelation into account when processing and analyzing their data.

Arbitrary aggregation schemes produce different results than more basic spatial units (i.e. ecoregions). In cases where fishnet and ecoregion polygons were of similar size on average (Level IV ecoregions and the 1,024km^2 fishnets, Level II ecoregions and the 65,536km^2 fishnets) (Table 1), the autocorrelation results were drastically different. Neither the Level II or Level IV ecoregions had significant autocorrelation (Level II $p = 0.9974$, Level IV $p = 0.3246$), while the corresponding fishnets all had significant autocorrelation regardless of polygon shape ($p = 2.20 \times 10^{-16}$ to 9.07×10^{-11}).

The results of the OLS models and LM/RLM tests illustrated that the MAUP had significant effects on spatial regressions. The fact that the best-suited model varied by polygon scale and shape indicates that the MAUP can affect the underlying relationships in the data. For example, there was no property intrinsic to the polygons where the optimal model was the spatial lag that should differentiate them as having high influence from spatial neighbors on the total area burned, nor as having more substantive spatial processes at work. Similarly, while the more frequent selection of spatial error models at larger aggregation scales may be indicative of the larger mismatch between data and process scale, the selection of the OLS model at the largest aggregation scale for all three fishnet styles calls this trend into question. This result may reflect an overall 'dilution' of the data from both non-federal land and no-data areas (i.e. areas outside of Western states) which becomes more apparent as the aggregation polygons become larger and both incorporate more non-federal land and extent further from the borders of the study area.

The emerging hotspot analysis results demonstrated that the effects of the MAUP extend beyond basic geospatial statistical tests and can influence temporal patterns.

Aggregating the data into triangles produced more sporadic hotspots than either of the other two aggregation schemes, but the aggregation did not have the same effect on consecutive or new hotspots. This result clearly indicates that the spatial aggregation of points has an effect on the occurrence of spatial hotspots and illustrates how that effect can affect temporal analyses.

The pattern of increasing variability in hotspot classification with aggregation scale is misleading. While variability increased with the aggregation scale, the number of polygons decreased, meaning that differences in smaller numbers of polygons produced larger changes in the classification percentages. In fact, while the 65,536km^2 polygons had the largest percentage variability in classification (4.56% on average), the spatial distribution of hotspots was very consistent.

Jelinski and Wu (1996) offered five solutions to dealing with the MAUP, of which two are more relevant to wildfire analyses. First, a sensitivity analysis can be used to measure which variables are most sensitive to the MAUP by testing different polygon calculations across a range of aggregation schemes. This approach requires very little time because producing aggregation polygons and running the analyses across different schemes is efficient with modern software and processors. Running a sensitivity analysis should be considered the bare minimum solution, as it can confirm or deny if the MAUP is significant, and guide further analyses based on the results. Second, a basic entity approach can be used to identify individual entities that are ecologically meaningful and not modifiable on which to perform analyses. Level IV ecoregions represent the basic areal units of landscape ecology and can thus be used in analyses to mitigate the MAUP. However, this approach is not sufficient in all cases as Level IV ecoregions have only been defined for the contiguous United States, and the size of the ecoregions may be too small for some applications.

There are also limitations to this study. First, quantifying which aggregation scale had the largest intra-scale variability is a difficult question. For example: Is a sporadic hotspot more similar to a new hotspot or a consecutive hotspot? What kind of hotspot is most different from no pattern? However, it is clear that the choice of aggregation polygon shape has an effect on the spatial distribution of hotspots in temporal analyses. Second, differences between the aggregation schemes may also vary with different temporal units used, especially given the importance of time to wildfire variables like fuel load accumulation and normal fire return intervals. The testing in this paper only encompassed temporal neighbors of 1 year, while wildfires have return intervals that can be much longer. Third, this study only explored the effects of the MAUP when aggregating wildfire data to regular isometric polygons. Future work is required to quantify the effects of the MAUP on other regular shapes (rectangles, isosceles triangles, etc.), or irregular polygons with equal or unequal areas. Finally, this study only used a few models to test the effects of MAUP. Additional future work could include analyses beyond those used in this study. For example, running a sensitivity analysis on a geographically weighted regression model would be a valuable contribution, as understanding the specific environmental factors that influence wildfire behavior is a critical goal of wildfire studies.

5. Conclusion

This study demonstrated that wildfire analyses are affected by the MAUP. Aggregating the same point data to different polygons changed basic summary

statistical measurements like Moran's I, to the extent that interpreting the results would lead to different understandings of the underlying processes in the data. Additionally, using different aggregation schemes also changed the more meta conclusions drawn from the Anselin model selection methodology. Thus, the influence of the MAUP is non-trivial and should be considered in similar studies. The MAUP also affected the results of a spatio-temporal analysis, further highlighting the need for judicial study design and aggregation scheme selection. For wildfire analysis is recommended that 1) a simple sensitivity analysis be run whenever wildfire point data are aggregated to quantify the magnitude of the MAUP, and 2) the basic spatial unit of ecology (Level IV ecoregions or equivalent) be used whenever possible to mitigate the effects of the MAUP.

References

Abatzoglou, J.T. & Williams, A.P. (2016). Impact of anthropogenic climate change on wildfire across western US forests. *Proceedings of the National Academy of Sciences*, *113*(42), 11770–11775. https://doi.org/10.1073/pnas.1607171113

Abt, K.L., Prestemon, J.P. & Gebert, K.M. (2009). Wildfire suppression cost forecasts for the US Forest Service. Journal of Forestry, 107(4), 173-178.

Ambrosia, V.G., Buechel, S.W., Brass, J.A., Peterson, J.R., Davies, R.H., Kane, R.J. & Spain, S. (1998). An integration of remote sensing, GIS, and information distribution for wildfire detection and management. *Photogrammetric Engineering and Remote Sensing*, *64*, 977–986.

Anselin, L. (1988). Lagrange multiplier test diagnostics for spatial dependence and spatial heterogeneity. *Geographical Analysis*, *20*(1), 1–17.

Anselin, L. (2003). Spatial externalities, spatial multipliers, and spatial econometrics. *International Regional Science Review*, *26*(2), 153–166.

Anselin, L. (2005). Exploring Spatial Data with GeoDa TM : A Workbook. *Geography*, 1–17.

Anselin, L. (2013). *Spatial econometrics: methods and models* (Vol. 4). Springer Science & Business Media.

Anselin, L. & Rey, S. (1991). Properties of Tests for Spatial Dependence in Linear Regression Models. *Geographical Analysis*, *23*(2), 112–131. https://doi.org/10.1111/j.1538-4632.1991.tb00228.x

Bailey, R.G. (1983). Delineation of ecosystem regions. *Environmental Management*, *7*(4), 365–373.

Bailey, R.G. (1995). *Ecosystem geography*. Springer.

Baller, R.D., Anselin, L., Messner, S.F., Deane, G. & Hawkins, D.F. (2001). Structural Covariates of U.S. County Homicide Rates: Incorporating Spatial Effects. *Criminology*, *39*(3), 561–588. https://doi.org/10.1111/j.1745-9125.2001.tb00933.x

Bartels, C.P.A. & Hordijk, L. (1977). On the power of the generalized Moran contiguity coefficient in testing for spatial autocorrelation among regression disturbances. *Regional Science and Urban Economics*, *7*(1–2), 83–101.

Brandsma, A.S. & Ketellapper, R.H. (1979). Further evidence on alternative procedures for testing of spatial autocorrelation among regression disturbances. In *Exploratory and explanatory statistical analysis of spatial data* (pp. 113–136). Springer.

Breusch, T.S. & Pagan, A.R. (1980). The Lagrange multiplier test and its applications to model specification in econometrics. *The Review of Economic Studies*, *47*(1), 239–253.

Calkin, D.E., Gebert, K.M., Jones, J.G., & Neilson, R.P. (2005). Forest Service large fire area burned and suppression. *Journal of Forestry*, *103*(4), 179–183.

Canadian Forest Service. (2018). *Canadian National Fire Database – Agency Fire Data*. Retrieved from http://cwfis.cfs.nrcan.gc.ca/ha/nfdb

Clark, W.A.V. & Avery, K.L. (1976). The Effects of Data Aggregation in Statistical Analysis. *Geographical Analysis*, *8*(4), 428–438. https://doi.org/10.1111/j.1538-4632.1976.tb00549.x

Collins, B.M., Omi, P.N. & Chapman, P.L. (2006). Regional relationships between climate and wildfire-burned area in the Interior West, USA. *Canadian Journal of Forest Research*, *36*(3), 699–709. https://doi.org/10.1139/x05-264

Dennison, P.E., Brewer, S.D., Arnold, J.D. & Moritz, M.A. (2014). Large wildfire trends in the western United States, 1984–2011. *Geophysical Prospecting*, *41*(8), 2928–2933. https://doi.org/10.1002/2014GL061184.Received

Di Luzio, M., Johnson, G.L., Daly, C., Eischeid, J.K. & Arnold, J.G. (2008). Constructing retrospective gridded daily precipitation and temperature datasets for the conterminous United States. *Journal of Applied Meteorology and Climatology*, *47*(2), 475–497. https://doi.org/10.1175/2007JAMC1356.1

Ecological Stratification Working Group. (1995). A National Ecological Framework for Canada. In *Environment*. https://doi.org/Cat. No. A42-65/1996E; ISBN 0-662-24107-X

Environmental Systems Research Institute. (2019a). *Create Space Time Cube By Aggregating Points*. Retrieved from https://pro.arcgis.com/en/pro-app/tool-reference/space-time-pattern-mining/create-space-time-cube.htm

Environmental Systems Research Institute. (2019b). *Emerging Hot Spot Analysis*. Retrieved from https://pro.arcgis.com/en/pro-app/tool-reference/space-time-pattern-mining/emerginghotspots.htm

Feltz, J.M., Moreau, M., Prins, E.M., McClaid-Cook, K. & Brown, I.F. (2003). Recent validation studies of the GOES wildfire automated biomass burning algorithm (WF_ABBA) in North and South America. *2nd Int. Wildland Fire Ecology Fire Management Congress, 5th Symp. Fire Forest Meteorology, Orlando, FL*.

Finco, M., Quayle, B., Zhang, Y., Lecker, J., Megown, K.A., & Brewer, C.K. (2012). Monitoring trends and burn severity (MTBS): monitoring wildfire activity for the past quarter century using Landsat data. *In: Morin, Randall S.; Liknes, Greg C., Comps. Moving from Status to Trends: Forest Inventory and Analysis (FIA) Symposium 2012; 2012 December 4-6; Baltimore, MD. Gen. Tech. Rep. NRS-P-105. Newtown Square, PA: US Department of Agriculture, Forest Service*, 222–228.

Fotheringham, A.S. & Wong, D.W.S. (1991). The modifiable areal unit problem in multivariate statistical analysis. *Environment and Planning A*, *23*, 1025–1044.

Fotheringham, A.S. (1989). Scale-independent spatial analysis. *Accuracy of Spatial Databases*, 221–228.

Fusco, E., Bradley, B. & Abatzoglou, J.T. (2018). Human-Related Ignitions Increase the Number of Large Wildfires across U.S. Ecoregions. *Fire*, *1*(1), 4. https://doi.org/10.3390/fire1010004

Fusco, E.J., Mahood, A.L., Balch, J.K., Bradley, B.A., Abatzoglou, J.T. & Nagy, R.C. (2017). Human-started wildfires expand the fire niche across the United States. *Proceedings of the National Academy of Sciences*, *114*(11), 2946–2951. https://doi.org/10.1073/pnas.1617394114

Getis, A. & Ord, J. K. (1992). *The Analysis of Spatial Association by Use of Distance Statistics, Geographycal Analysis, 24*.

Getis, A. & Ord, J.K. (1995). Local Spatial Autocorrelation Statistics: Distributional Issues and an Application. *Geographical Analysis*, *27*(4), 286–306. https://doi.org/10.1111/j.1538-4632.1995.tb00912.x

Gralewicz, N.J., Nelson, T.A. & Wulder, M.A. (2012). Spatial and temporal patterns of wildfire ignitions in Canada from 1980 to 2006. *International Journal of Wildland Fire*, *21*(3), 230–242. https://doi.org/10.1071/WF10095

Harris, A.J.L. (1996). Towards Automated Fire Monitoring From Space: Semi-Automated Mapping of the January 1994 New South Wales Wildfires Using AVHRR Data. *International Journal of Wildland Fire*, *6*(3), 107–116.

Jelinski, D.E. & Wu, J. (1996). The modifiable areal unit problem and implications for landscape ecology. *Landscape Ecology*, *11*(3), 129–140. https://doi.org/10.1007/BF02447512

Jiang, Y. & Zhuang, Q. (2011). Extreme value analysis of wildfires in Canadian boreal forest ecosystems. *Canadian Journal of Forest Research*, *41*(9), 1836–1851. https://doi.org/10.1139/x11-102

Jiang, Y., Zhuang, Q., Flannigan, M.D. & Little, J.M. (2009). Characterization of wildfire regimes in Canadian boreal terrestrial ecosystems. *International Journal of Wildland Fire*, *18*(8), 992. https://doi.org/10.1071/wf08096

Joseph, M.B., Rossi, M.W., Mietkiewicz, N.P., Mahood, A.L., Cattau, M.E., Denis, L.A. St., … Balch, J.K. (2018). Understanding and predicting extreme wildfires in the contiguous United States. *BioRxiv*, 384115. https://doi.org/10.1101/384115

Kendall, M.G. & Gibbons, J.D. (1990). Rank Correlation Methods, fifthed. *Griffin, London, UK*.

Koltunov, A., Ustin, S.L. & Prins, E.M. (2012). On timeliness and accuracy of wildfire detection by the GOES WF-ABBA algorithm over California during the 2006 fire season. *Remote Sensing of Environment*, *127*, 194–209.

Krawchuk, M.A., Moritz, M.A., Parisien, M.A., Van Dorn, J. & Hayhoe, K. (2009). Global pyrogeography: The current and future distribution of wildfire. *PLoS ONE*, *4*(4). https://doi.org/10.1371/journal.pone.0005102

Legendre, P. (1993). Spatial autocorrelation: trouble or new paradigm? *Ecology*, *74*(6), 1659–1673.

Litschert, S.E., Brown, T.C. & Theobald, D.M. (2012). Historic and future extent of wildfires in the Southern Rockies Ecoregion, USA. *Forest Ecology and Management*, *269*, 124–133. https://doi.org/10.1016/j.foreco.2011.12.024

Malamud, B.D., Millington, J. D.A. & Perry, G.L.W. (2005). Characterizing wildfire regimes in the United States. *Proceedings of the National Academy of Sciences*, *102*(13), 4694–4699. https://doi.org/10.1073/pnas.0500880102

Mann, H.B. (1945). Nonparametric tests against trend. *Econometrica: Journal of the Econometric Society*, 245–259.

McMahon, G., Gregonis, S.M., Waltman, S.W., Waltman, S.W., Omernik, J.M., Omernik, J.M., … Keys, J.E. (2001). Developing a Spatial Framework of Common Ecological Regions for the Conterminous United States. *Environmental Management*, *28*(3), 293–316. https://doi.org/10.1007/s002670010225

Miller, J., Borne, K., Thomas, B., Huang, Z., & Chi, Y. (2013). Automated wildfire detection through artificial neural networks. In *Remote Sensing and Modeling Applications to Wildland Fires* (pp. 293–304). Springer.

Moran, P.A.P. (1950). Notes on continuous stochastic phenomena. *Biometrika*, *37*(1/2), 17–23.

Moreno, M.V., Malamud, B.D. & Chuvieco, E. (2011). Wildfire frequency-area statistics in Spain. *Procedia Environmental Sciences*, *7*, 182–187. https://doi.org/10.1016/j.proenv.2011.07.032

Omernik, J. M. (1987). Ecoregions of the conterminous United States. *Annals of the Association of American Geographers*, *77*(1), 118–125.

Omernik, J.M. (2004). Perspectives on the Nature and Definition of Ecological Regions. *Environmental Management*, *34*(S1), S27–S38. https://doi.org/10.1007/s00267-003-5197-2

Omernik, J.M. & Griffith, G.E. (2014). Ecoregions of the Conterminous United States: Evolution of a Hierarchical Spatial Framework. *Environmental Management*, *54*(6), 1249–1266. https://doi.org/10.1007/s00267-014-0364-1

Openshaw, S. (1984). The modifiable areal unit problem. *Concepts and Techniques in Modern Geography*.

Openshaw, S. & Taylor, P. (1981). *Quantitative Geography: A British View, chapter The Modifiable Areal Unit Problem*. London: Routledge.

Perle, E.D. (1977). Scale changes and impacts on factorial ecology structures. *Environment and Planning A*, *9*(5), 549–558.

Prestemon, J.P., Abt, K. & Gebert, K. (2008). Suppression cost forecasts in advance of wildfire seasons. *Forest Science*, *54*(4), 381–396.

Prins, E.M., Schmidt, C.C., Feltz, J.M., Reid, J.S., Westphal, D.L. & Richardson, K. (2003). *A two-year analysis of fire activity in the western hemisphere as observed with the GOES wildfire automated biomass burning algorithm*.

Schoennagel, T., Balch, J.K., Brenkert-Smith, H., Dennison, P.E., Harvey, B.J., Krawchuk, M.A., … Whitlock, C. (2017). Adapt to more wildfire in western North American forests as climate changes. *Proceedings of the National Academy of Sciences*, *114*(18), 4582–4590. https://doi.org/10.1073/pnas.1617464114

Short, K.C. (2017). *Spatial wildfire occurrence data for the United States, 1992-2015 [FPA_FOD_20170508]*.

Sokal, R.R. & Oden, N.L. (1978). Spatial autocorrelation in biology: 1. Methodology. *Biological Journal of the Linnean Society*, *10*(2), 199–228.

United States Department of Interior. (2018). *The Federal Fire Occurrence Database*. Retrieved from https://wildfire.cr.usgs.gov/firehistory/data.html

United States Environmental Protection Agency. (2016a). *Ecoregions of North America*. Retrieved from https://www.epa.gov/eco-research/ecoregions-north-america

United States Environmental Protection Agency. (2016b). *Level III and IV Ecoregions of the Continental United States*. Retrieved from https://www.epa.gov/eco-research/level-iii-and-iv-ecoregions-continental-united-states

Vincent, C.H., Hanson, L.A. & Argueta, C.N. (2017). Federal Land Ownership: Overview and Data Carol Hardy Vincent Specialist in Natural Resources Policy Analyst in Immigration Policy. *Congressional Research Service*, 28. Retrieved from https://fas.org/sgp/crs/misc/R42346.pdf

Westerling, A.L., Hidalgo, H.G., Cayan, D.R. & Swetnam, T.W. (2006). Warming and earlier spring increase Western U.S. forest wildfire activity. *Science*, *313*(5789), 940–943. https://doi.org/10.1126/science.1128834